G. Z. Wang
e-mail: guozhong.wang@daimlerchyrsler.com

Z. N. Cheng
e-mail: zhaonian.cheng@daimlerChrysler.com

Daimler Chrysler SIM Technology,
865 Changning Road,
Shanghai 200050, China

K. Becker
University of Applied Science Bingen,
Bingen 55411, Germany
e-mail: becker@fh-bingen.de

J. Wilde
IMTEK, University of Freiburg,
Freiburg im Breisgan D-79085, Germany
e-mail: wilde@imtek.uni-freiburg.de

Applying Anand Model to Represent the Viscoplastic Deformation Behavior of Solder Alloys

A unified viscoplastic constitutive law, the Anand model, was applied to represent the inelastic deformation behavior for solders used in electronic packaging. The material parameters of the constitutive relations for 62Sn36Pb2Ag, 60Sn40Pb, 96.5Sn3.5Ag, and 97.5Pb2.5Sn solders were determined from separated constitutive relations and experimental results. The achieved unified Anand model for solders were tested for constant strain rate testing, steady-state plastic flow and stress/strain responses under cyclic loading. It is concluded that the Anand model can be applied for representing the inelastic deformation behavior of solders at high homologous temperature and can be recommended for finite element simulation of the stress/strain responses of solder joints in service. [DOI: 10.1115/1.1371781]

Introduction

In general, temperature fluctuations experienced by IC packages and assemblies in service cause progressive damage in solder joints; eventually, this damage accumulation beyond certain limits leads to the electrical failure. One of the major goals of thermomechanical analysis in the electronics industry is to be able to simulate the stress/strain responses of the solder joint and then predict its reliability in service. In order to gain accurate simulation and reliable prediction, realistic constitutive relations for solder alloys are warranted.

The high homologous temperatures, e.g., 0.65 T_m (in K) for the eutectic tin-lead(SnPb) at room temperature, experienced by the solder joint and the thermally activated strains imposed on it due to the thermal expansion mismatch between the materials gives rise to a complex deformation behavior. This deformation behavior is associated with the irreversible, temperature and rate (or time) dependent inelastic characteristics, producing strain-hardening, dynamic recovery, and in many instances dynamic recrystallization. This deformation behavior is known to be viscoplastic with, generally, revelations such as creep and stress relaxation phenomena of materials working in high homologous temperature regime.

There has already been a great deal of effort applied to reasonable experimental data and constitutive models for this material. The previous researchers (Darveaux and Banerji [1]; Weinbel et al. [2], Kashyap and Murty [3]) presented extensive experimental data on tin-lead based solders. There are also some constitutive relations for solder alloys, ranging from elasto-plastic model (e.g., Ramberg-Osgood relation) using empirical stress-strain curves (Lau and Rice [4]) to a purely phenomenological model where the time-dependent and time-independent deforms are artificially separated (Sarihan [5], Pao et al. [6]; Knecht and Fox [7]). Some creep models from literature (power law creep, Harper Dorn creep, hyperbolic sine creep, etc.) have been applied to the time dependent creep data. However, from the viewpoint of continuum mechanics, the time-dependent and time-independent inelastic strains are assumed to arise from similar mechanisms due to dislocation motion. So, a unified framework for viscoplastic behavior of solder materials is highly desired. However, there exist insufficient works until now. Some researches (Busso et al. [8], Busso and Kitano [9]) proposed a unified model for 60Sn40Pb solder which accounts for the measured stress-dependence of the activation energy and for the Bauschinger effect exhibited by the solder. Qian et al. [10] employed the back stress to describe the transient stage of a stress/strain curve in a unified constitutive model for tin-lead solder. Some works (Skipor et al. [11]; Ma et al. [12]) employed the Bodner-Partom constitutive relations which use a state variable to represent the internal inelastic structure for the solder with eutectic composition. However, some parameters of these unified models are empirical and dependent on temperature and strain rate, resulting in complex calculation of the stress strain responses and some scattering predictions from the experiments.

Usually, a specially viscoplastic constitutive law must be defined as a user-defined subroutine code to represent the nonlinear rate-dependent stress-strain relations in some finite element programs (Busso et al. [8], Qian et al. [10]). Such a work is often complex, expert dependent and largely time consumptive. Some user material subroutines with unified constitutive models are already available in current commercial finite element codes, e.g., the UMAT in ABAQUS (Weber et al. [13]). A unified constitutive model, which is referred to as the Anand model, is offered by the ANSYS code. In order to apply this Anand model to simulating the thermomechanical responses of solder joints in electronic packaging, the material parameters of the constitutive relations must be determined in prior.

The objective of this paper is to obtain the material parameters of the Anand model for solders from experimental results and the separated elasto-plasto-creep constitutive relations. The material parameters with viscoplastic constitutive relations for solders are used to simulate the steady-state creep behavior, constant strain rate behavior, and stress/strain responses under thermal cyclic loading for comparison and verification. Some discussions on recommendation of using unified Anand model in the finite element simulation of electronic packaging reliability were also presented.

Model Formulation

1 The Anand Model. A simple set of constitutive equations for large, isotropic, viscoplastic deformations but small elastic deformations is the single-scalar internal variable model proposed by Anand and Brown (Anand [14], Brown et al. [15]). There are two basic features in this Anand model. First, this model needs no explicit yield condition and no loading/unloading criterion. The plastic strain is assumed to take place at all nonzero stress values, although at low stresses the rate of plastic flow may be immea-

Contributed by the Electronic and Photonic Packaging Division for publication in the JOURNAL OF ELECTRONIC PACKAGING. Manuscript received by the EPPD October 20, 1998. Associate Editor: Ye-Hein Pao.

surably small. Second, this model employs a single scalar as an internal variable to represent the isotropic resistance to plastic flow offered by the internal state of the material. This internal variable is denoted by s, which has the dimensions of stress, and is called to be deformation resistance. There are some reasonable considerations for the simplifications that only a single scalar is used to characterize the internal structural characteristics of a material (Brown et al. [15]). The set of Anand constitutive equations presented here accounts for the physical phenomena of strain-rate and temperature sensitivity, strain rate history effects, strain-hardening and the restoration process of dynamic recovery.

The internal variable s represents an averaged isotropic resistance to macroscopic plastic flow offered by the underlying isotropic strengthening mechanisms such as dislocation density, solid solution strengthening, subgrain, and grain size effects, etc. The deformation resistance s is consequently proportional to the equivalent stress σ. That is

$$\sigma = c \cdot s; \; c < 1 \tag{1}$$

where c is a material parameter and constant in the constant strain rate test, which is defined as

$$c = \frac{1}{\xi} \sinh^{-1}\left[\left(\frac{\dot{\varepsilon}_P}{A} e^{Q/RT}\right)^m\right] \tag{2}$$

where $\dot{\varepsilon}_P$ is the inelastic strain rate, A is the pre-exponential factor, Q is the activation energy, m is the strain rate sensitivity, ξ is the multiplier of stress, R is the gas constant, and T is the absolute temperature, respectively.

The following functional form of the flow equation was selected to exactly accommodate the strain rate dependence on the stress at constant structure:

$$\dot{\varepsilon}_P = A \exp\left(-\frac{Q}{RT}\right)\left[\sinh\left(\xi\frac{\sigma}{s}\right)\right]^{1/m} \tag{3}$$

Note that the internal state variable enters into the flow equation only as a ratio with the equivalent stress. The temperature dependence in Eq. (3) is incorporated via a classical Arrhenius term. While the stress and state dependence is a simple modification of the hyperbolic sine form first proposed by Garofalo [16] to model steady-state plastic flow (secondary creep).

The evolution equation for the internal variable s is assumed to be of the form as

$$\dot{s} = g(\sigma, s, T)\dot{\varepsilon}_P \tag{4}$$

where the function $g(\sigma, s, T)$ is associated with dynamic process, that is, strain hardening and dynamic recovery. A simple form of evolution equation of Eq. (4) was given by Anand [14] as follows:

$$\dot{s} = \left\{ h_0 \left| 1 - \frac{s}{s^*} \right|^a \cdot sign\left(1 - \frac{s}{s^*}\right)\right\} \cdot \dot{\varepsilon}_P; \; a > 1 \tag{5}$$

with

$$s^* = \hat{s}\left[\frac{\dot{\varepsilon}_P}{A}\exp\left(\frac{Q}{RT}\right)\right]^n \tag{6}$$

where h_0 is the hardening/softening constant, a is the strain rate sensitivity of hardening/softening. The quantity s^* represents a saturation value of s associated with a set of given temperature and strain rate as shown in Eq. (6). $\hat{s}$ is a coefficient, and n is the strain rate sensitivity for the saturation value of deformation resistance, respectively.

From the above viscoplastic Anand model, there are nine material parameters: $A, Q, \xi, m, h_0, \hat{s}, n, a$, and s_0, the last one is the initial value of the deformation resistance, which is needed to determine the evolution of deformation resistance in Eq. (5).

2 The Separated Constitutive Model. In the separated constitutive descriptions for solder alloys, the total inelastic strain γ is the sum of time-independent plastic strain γ_P, the steady-state creep γ_S, and the transient (or primary) creep strain γ_T. That is

$$\gamma = \gamma_P + \gamma_S + \gamma_T \tag{7}$$

with

$$\gamma_P = C_2\left(\frac{\tau}{G}\right)^{m_p} \tag{8}$$

$$\gamma_S = \dot{\gamma}_S \cdot t \tag{9}$$

$$\gamma_T = \gamma_t[1 - \exp(-B\dot{\gamma}_S t)] \tag{10}$$

where τ is the applied shear stress, G is the shear modulus, C_2 is the plastic strain coefficient, m_p is the stress sensitivity of plastic strain, $\dot{\gamma}_S$ is the steady-state strain rate. B is the transient creep coefficient, γ_t is the transient creep strain, and t is the time, respectively.

The steady-state creep rate can be described by a single expression, a hyperbolic sine form from Darveaux and Baneji [1]. That is

Table 1 Material parameters of separated model for solders (Darveaux and Banerji [1])

	Elastic		Steady State Creep[2]				Transient Creep		Plastic[2]	
Solder	G_0 (at 0°SC) (10^4MPa)	G_1 (10^2MPA)	C_1 (K/s/MPa)	α	n_S	Q (ev)	B	γ_t	C_2	m_p
60Sn40Pb										
Shear	1.310	0.559	28.720	1300	3.3	0.548	440	0.020	$2.3(10^{13})$	5.6
Tensile[1]	3.447	1.517	16.534	751	3.3	0.548	762	0.012	$6.1(10^{11})$	5.6
62Sn36Pb2Ag										
Shear	1.310	0.559	14.344	1300	3.3	0.548	137	0.037	$6.6(10^{7})$	4.5
Tensile[1]	3.447	1.517	8.282	751	3.3	0.548	237	0.021	$5.6(10^{6})$	3.5
96.5Sn3.5Ag										
Shear	1.931	0.689	$7.09(10^{-2})$	1300	5.5	0.40	147	0.086	$2.0(10^{11})$	4.4
Tensile[1]	5.240	1.931	$4.09(10^{-2})$	751	5.5	0.40	255	0.050	$1.0(10^{10})$	4.4
97.5Pb2.5Sn										
Shear	0.896	0.103	$7.31(10^{9})$	1200	7.0	1.20	137	0.115	$2.8(10^{10})$	4.0
Tensile[1]	2.413	0.283	$4.22(10^{9})$	693	7.0	1.20	237	0.066	$1.8(10^{9})$	4.0

[1]Inelastic tensile constants derived from shear constants using relations $\sigma = \tau\sqrt{3}$ and $\varepsilon = \gamma/\sqrt{3}$ due to the assuming of von Mises yield criteria.
[2]Use shear modulus when calculating tensile strain rate in Eq. (11) and plastic strain in Eq. (8).

$$\dot{\gamma}_S = C_1 \frac{G}{T}\left[\sinh\left(\alpha\frac{\tau}{G}\right)\right]^{n_s}\exp\left(-\frac{Q}{RT}\right) \tag{11}$$

where C_1 is a coefficient, α is the multiplier of stress, and n_s is the stress sensitivity of steady-state creep rate, respectively. A hyperbolic sine dependence of the strain rate on the stress results from an assumption of forward and backward thermal activation of vacancies. However, some investigators (Arrowood et al. [17]) associated power law breakdown with a transition from dislocation climb dominated steady-state plastic flow to dislocation glide dominated one.

To obtain the total inelastic strain, the temperature dependence of the shear modulus G must be incorporated

$$G = G_0 - G_1 \cdot T(^\circ\mathrm{C}) \tag{12}$$

where G_0 is the shear modulus 0°C, and G_1 gives the temperature dependence. Table 1 lists the material parameters of the separated elasto-plasto-creep model for 60Sn40Pb, 62Sn36Pb, 96.5Sn3.5Ag, and 97.5Pb2.5Sn solders.

Parameters Determination of Anand Model

1 Steady-State Plastic Flow and Saturation Stress. When steady-state plastic flow occurs, the stress reaches the saturation value. For viscoplastic deformation behavior, this steady-state plastic flow happens when the plastic flow has become fully developed and its rate equals the applied strain rate at the given temperature and strain rate. The steady-state plastic flow of Anand model can be derived as

$$\dot{\varepsilon}_P = \dot{\varepsilon} = A\exp\left(-\frac{Q}{RT}\right)\left[\sinh\xi\frac{\sigma^*}{s^*}\right]^{1/m} \tag{13}$$

where $\dot{\varepsilon}$ is the applied strain rate in constant strain rate test. From Eq. (13), the saturation stress σ^* is obtained as follows:

$$\sigma^* = cs^* = \frac{\hat{s}}{\xi}\left(\frac{\dot{\varepsilon}_p}{A}e^{Q/Rt}\right)^n \sinh^{-1}\left[\left(\frac{\dot{\varepsilon}_p}{A}e^{Q/RT}\right)^m\right] \tag{14}$$

From the above, the material parameters: $Q/R, A, \hat{s}/\xi, m$ and n in Eq. (14) can be determined by applying a nonlinear fitting method using $\dot{\varepsilon}_p \sim \sigma^*$ pair data from steady-state creep results.

2 Determination Procedures and Results. The material parameters of the elastic, plastic, and creep deformation behavior shown in Table 1 can be transformed to the viscoplastic Anand model. The values of the nine material parameters $A, Q, \xi, m, h_0, a, \hat{s}$, and n for any given solder alloy were determined by following the procedures outlined below:

(a) Determination of the saturation stresses σ^* under strain rates $\dot{\varepsilon}$ and temperatures T from steady-state creep relation.

(b) Nonlinear fitting of $Q/R, A, \hat{s}/\xi, m$ and n in Eq. (14).

Table 2 Material parameters of viscoplastic Anand model for solders

Material Parameters	Solders			
	60Sn40Pb	62Sn36Pb2Ag	96.5Sn3.5Ag	97.5Pb2.5Sn
A (s^{-1})	1.49(10^7)	2.30(10^7)	2.23(10^4)	3.25(10^{12})
Q/R (°K)	10830	11262	8900	15583
ξ	11	11	6	7
m	0.303	0.303	0.182	0.143
$\hat{s}$ (MPa)	80.42	80.79	73.81	72.73
n	0.0231	0.0212	0.018	0.00437
h_0 (MPa)	2640.75	4121.31	3321.15	1787.02
a	1.34	1.38	1.82	3.73
s_0 (MPa)	56.33	42.32	39.09	15.09

(c) Determination of ξ and $\hat{s}$. By using the values obtained in step (b), the parameter ξ was slected such that the constant c in Eq. (2) is less than unity, and $\hat{s}$ was then determined from the combined term $\hat{s}/\xi$.

(d) Nonlinear fitting of a, h_0 and s_0. The stress of Anand model can be expressed as

$$\sigma = \sigma^* - [(\sigma^* - cs_0)^{(1-a)} + (a-1)\{(ch_0)(\sigma^*)^{-a}\}\varepsilon_p]^{1/(1-a)} \tag{15}$$

The material parameters a, h_0, and s were fitted from the $\sigma \sim \varepsilon_P$ curves (especially the transient state) with various temperatures and strain rates. In the fitting, the saturation stresses given in step (*a*) were also used.

The nine material parameters for 62Sn36Pb2Ag, 60Sn40Pb, 96.5Sn3.5Ag, and 97.5Pb2.5Sn solder materials, determined from the above procedure, are listed in Table 2. For a whole deformation response for solder due to a load, the elastic behavior should also be included. The elastic properties, e.g., the temperature dependent elastic moduli, for these solders are the same as listed in Table 1. The Poisson's ratios can also be derived from the relationship between shear modulus and tensile modulus in Table 1.

Verification and Application

1 Model Prediction. The achieved material parameters of unified Anand model for solders were tested for constant strain

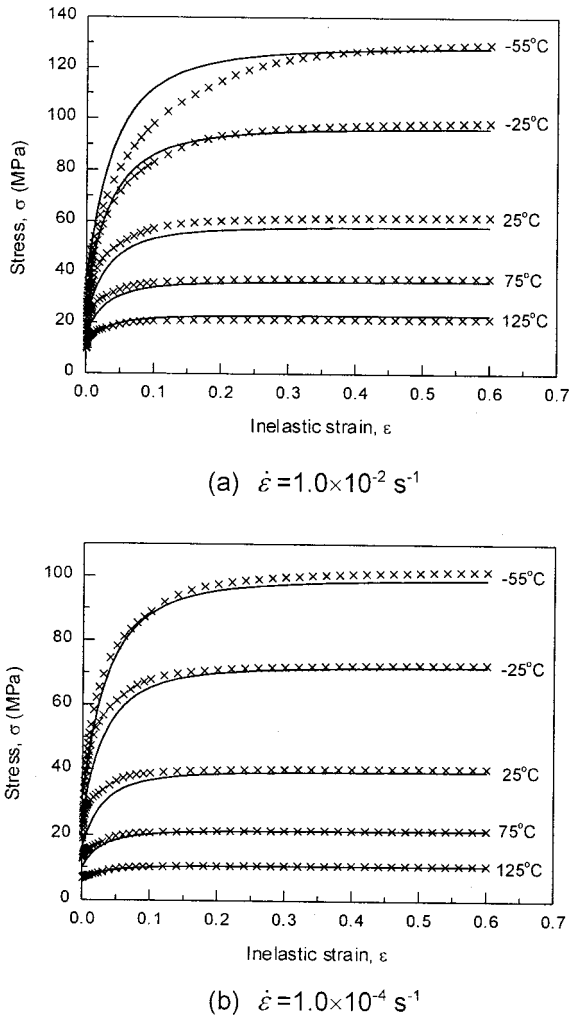

Fig. 1 Constant strain rate behavior of 60Sn40Pb solder (×: derived from elasto-plasto-creep model; —: prediction from Anand model)

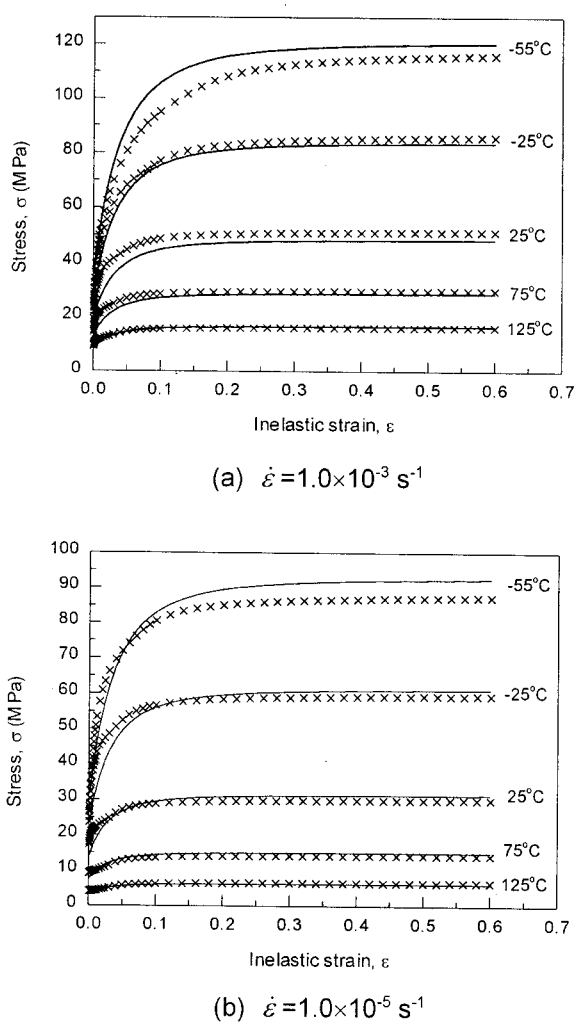

Fig. 2 Constant strain rate behavior of 62Sn36Pb2Ag solder (×: derived from elasto-plasto-creep model; —: prediction from Anand model)

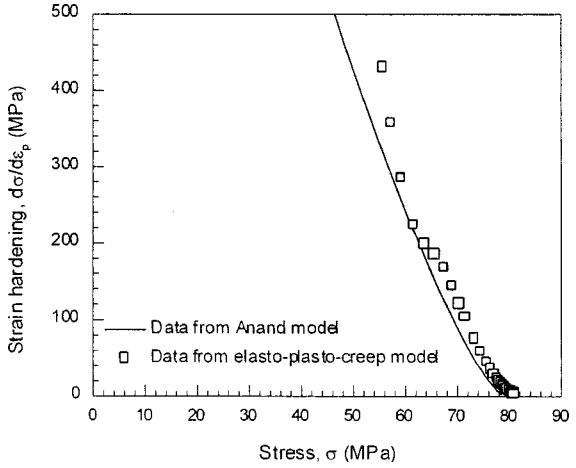

Fig. 3 Plastic strain hardening data for 60Sn40Pb solder ($\dot{\varepsilon}=1.0\times10^{-3}$ s^{-1}, T=−25°C)

rate behavior and steady-state plastic flow. The temperature of the constant strain rate behavior ranges from −55°C–+125°C and the strain rate ranges from 1.0×10^{-2}s^{-1}–1.0×10^{-5}s^{-1}. As the representative results, Fig. 1 and Fig. 2 illustrate the comparisons between the stress-strain data derived from separated model and the prediction results from Anand model for 60Sn40Pb and 62Sn36Pb2Ag solders, respectively. A good agreement between the model predictions and the data from separated model is achieved for the above conditions, especially in the regimes where the steady-state plastic flow apparently occurs. Also, the temperature and strain rate dependence of the onset of plastic flow, and the general features of the strain hardening behavior of the stress-strain curves can be clearly seen from these figures. One can also see there are some small differences in the transients (the nonsteady-state segments in the stress-strain response). Nevertheless, the Anand model represents the deformation behavior quite well.

Under isothermal and constant strain rate conditions, for plastic flow not developed fully, i.e., $s<s^*$, the strain hardening data $d\sigma/d\varepsilon_p$, that is the slope of the stress versus inelastic strain curve, can be represented as

$$\frac{\sigma}{d\varepsilon_p}=ch_0\left(1-\frac{s}{s^*}\right)a \tag{16}$$

The strain hardening data reflects the rate sensitivity and the evolution of the internal variable. Based on Eq. (16), the hardening data can then be calculated. Figure 3 shows the relationship between $d\sigma/d\varepsilon_p$ and σ data of 60Sn40Pb solder at temperature −25°C and strain rate 1.0×10^{-3}s^{-1}. The corresponding data based on the separated model were also calculated and plotted in this figure. It is seen that although the Anand model underestimates the strain hardening at low stresses, both models produce the coincident results.

As independent verification is provided by steady-state creep data. The steady-state creep rates of 60Sn40Pb and 96.5Sn3.5Ag solders from experiments of Darveaux and Banerji [1] and the model predictions are plotted versus shear stresses in Fig. 4(*a*) and Fig. 5, respectively. Figure 4(*b*) also shows another independent verification of creep data for 60Sn40Pb solder around room temperature reported in the literature (Grivals et al. [18], Solomon [19], Busso and Kitano [9]). Both Fig. 4 and 5 indicated that the experimental data and the prediction results are coincident well. Also, the model predictions capture the characteristic of the power law breakdown for steady-state creep behavior.

2 Steady-State Creep Approximation. One can find the flow equation (Eq. (3)) of Anand model follows the same hyperbolic sine form of the secondary creep law (Eq. (11)) with modification of internal state variable as denominator in the stress term, together with providing an evolution equation for the state variable. In electronic packaging applications, because the steady-state creep deformation processes dominated the deformation kinetics of solder alloys due to their low melting point (Frost and Ashby [11]), the material model for inelastic response of solders is often treated as steady-state creep (to name a few, Holden and Wallach [20], Wang et al. [21], Hong and Burrell [22]). Therefore, it is interesting to use the Anand model to represent the steady-state plastic flow of solders.

As mentioned above, the steady-state plastic flow occurs when the deformation resistance s, equals the saturation value s^* (see Eq. (13)). Then, the evolution equation can be skipped and there is no hardening/softening effect, the hardening/softening constant is given a value of zero, i.e., $h_0=0$ and its strain rate sensitivity $a=1$. The strain rate sensitivity for saturation s^* is also set to be zero, i.e., $n=0$, resulting parameters s_0 and $\hat{s}$ possess the same values as s^*. Thereafter, the Anand model is simplified to the hyperbolic sine creep form. Some researchers (Wiese et al. [23], Fusaro and Darveaux [24]) have already used this rate dependent model to represent the hyperbolic sine steady-state creep of solders.

Moreover, the Anand model can also be simplified to be the power law creep form. The secondary creep of solders associated with Norton's equation is

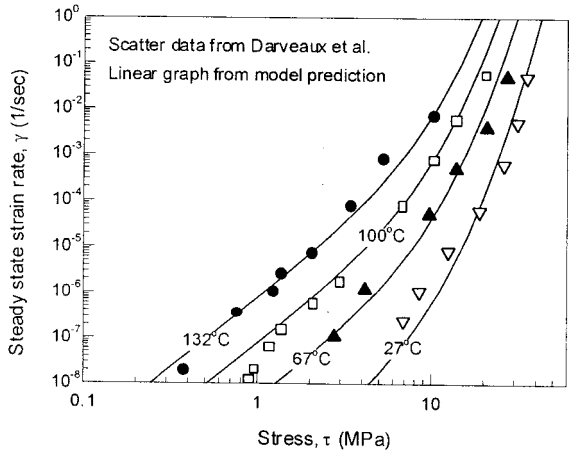

(a)

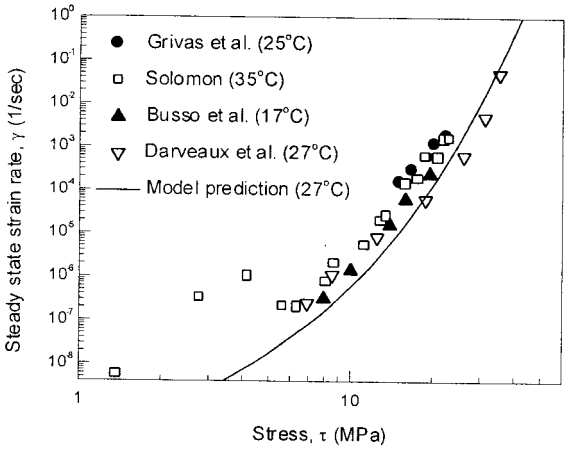

(b)

Fig. 4 Steady-state creep behavior of 60Sn40Pb solder

$$\dot{\gamma}_S = B^* \exp\left[\frac{-\Delta H}{kT}\right]\tau^{n*} \tag{17}$$

where B^* is a material constants, ΔH is the activation energy, k is the Boltzmann's constant, and n^* is the stress component. The creep properties of eutectic SnPb are determined (Pao et al. [25])

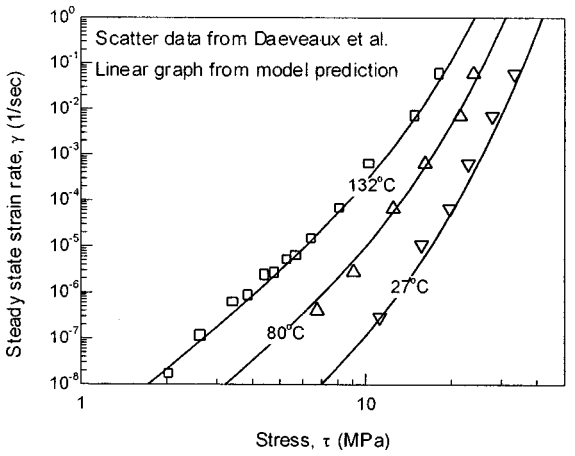

Fig. 5 Steady-state creep behavior of 96.5Sn3.5Ag solder

Table 3 Material parameters with Anand model of 60Sn40Pb solder for power law steady-state creep approximation

A	Q/R	ξ	m	$\hat{s}$	n	h_0	a	s_0
$2.09(10^8)$	5686	1	0.019	100	0	0	1	100

to be: $B^* = 0.205$ 1/MPa^{n}s, $\Delta H = 0.49$ ev, and $n^* = 5.25$. Because the stresses induced in solder joints for electronic packaging applications are usually less than 100 MPa, with an additional consideration to let the condition $\xi/s^* = 1/100$, then the flow equation of the Anand model has the same power law representation. The obtained material parameters are listed in Table 3.

3 A Simple Application Example. The viscoplastic Anand model has been previously used to finite element simulate the stress/strain responses of solder joints of some electronic packages, e.g., a chip scale assembly (Wilde et al. [26]). Here, only a simple specimen was selected to perform the simulations. The specimen is composed of two elastic beams, the Al_2O_3 ceramic and FR4 substrate, clamping with solder sandwiched at both ends, which is similar to the Ford joint specimen (Pao et al. [27]), as shown in Fig. 6. Moreover, the unified constitutive framework was also simplified to power law steady-state creep (hereafter, referred to as Anand approximation model). The 60Sn40Pb solder was selected to form the solder joints. A power law creep model was also utilized in the simulation to clarify the differences of stress/strain responses in the solder joint under thermal cycling. The corresponding material constants for both models were presented in the above Section.

Due to the symmetrical geometry, only half of the specimen was meshed with 2D plane strain elements. In the simulation with the Anand approximation model, the material parameters were defined in the ANSYS and a viscous element type (visco106) was selected for the solder. Table 4 lists the elastic properties of the involved materials. The temperature of thermal cycling ranged from −55°C–+125°C with ramp rate of 36°C/min and dwell time of 10 min at the two temperature extremes. The reference temperature was treated as 125°C.

Figure 7 shows the simulation results of inelastic shear stain distributions in solder joints at the start of the −55°C dwell of the third thermal cycle based on both models. The results show that the strain distributions based on both models are coincident well. The inner lower corner near the solder/FR4 interface demonstrates the strain localization and may be the potential failure site. Traditionally, the prediction on thermal fatigue life of solder joint is

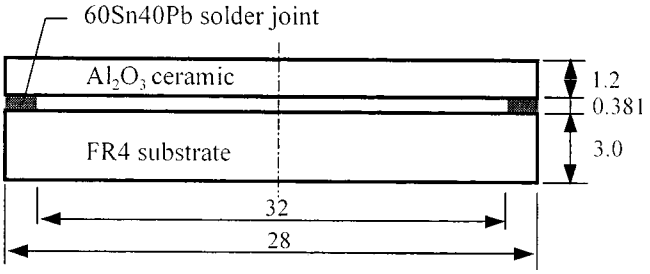

Fig. 6 Schematic diagram of a simple specimen

Table 4 Elastic mechanical properties of materials

Materials	Young's modulus (MPa)	Poisson's ratio	Coefficient of thermal expansion (ppm/°C)
60Sn40Pb	$3.447(10^4) - 151.7T(°C)$	0.316	25
Al_2O_3	$2.76(10^5)$	0.3	6.7
FR4	$1.6(10^4)$	0.3	16

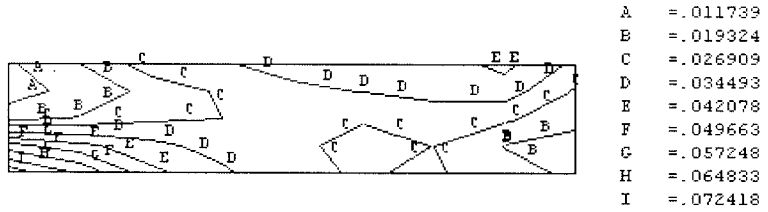

(a) based on power law creep model

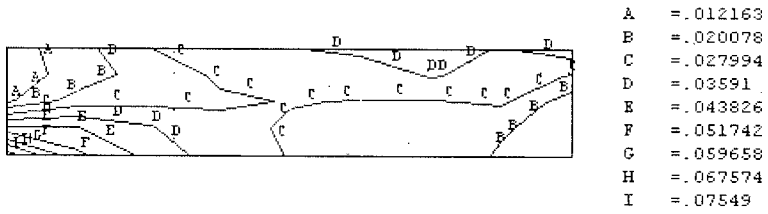

(b) based on Anand approximation model

Fig. 7 Distributions of inelastic shear strains in solder joints at start −55°C dwell of the third thermal cycle

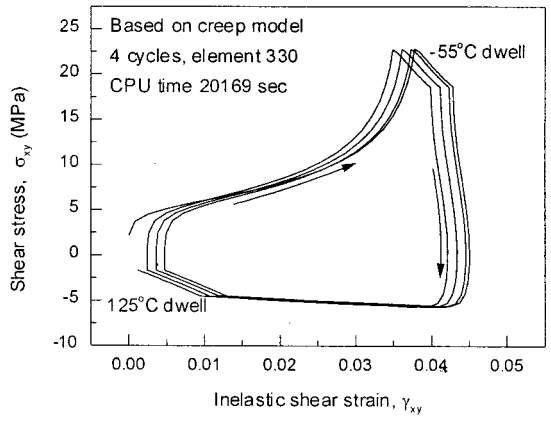

(a)

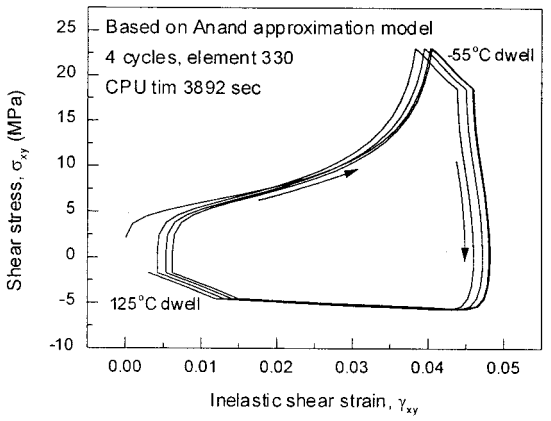

(b)

Fig. 8 Stress-strain hysteresis loops of the selected element in solder joints under thermal cycling

based on the estimation of failure indicator such as the cyclic inelastic strain range through Coffin-Manson empirical equation and its modified forms. The cyclic strain range can be obtained from the stress-strain hysteresis loops. The hysteresis loops of a element 330 close to the inner lower corner with strain localization based on the two models are shown in Fig. 8. It is seen that the hysteresis loops follow the same cyclic pattern, and the thermal cycle lifetimes can then be assumed approximately the same due to almost the same inelastic strain ranges.

It is found that the CPU time (3892 s) of finite element simulations for 4 thermal cycles with Anand model is greatly less than that (20169 s) with creep model for the same precision in the simple application. Finite element analysis of highly nonlinear problems is generally very CPU time-consumption as the structure stiffness matrix must be updated during each time step. The creep equations are integrated with an explicit Euler forward algorithm in ANSYS software, which is only efficient for problems having small amounts of contained creep strains (0.25%). Since an explicit integration procedure is used, a stability is placed on the time step size according to the creep ratio, a measure of the increment of creep strain. It is recommended to use a time step size such that the creep ratio is less than 0.1. Therefore, the simulation for problems dominated by creep, is very time-consumption. The integration of the flow equation for the Anand model is, however, run with an Euler backward algorithm. A consistent stress update procedure which is equivalent to the backward Euler scheme is used to enforce the consistency condition and the evolution equation at the end of the time step. Hence, the CPU time of simulation can be reduced considerably with no strict stability limit.

Discussions

Due to the above results, the unified Anand model can be applied for representing the inelastic deformation of solders. This model can also be conveniently used and should be recommended in finite element simulation of stress/strain responses of solder joints in service. The reasons are as follows:

(a) *A unified framework for solder behavior*. Currently, the constitutive models of solder alloys, used in electronic packaging,

are mostly separated as rate independent plasticity and steady-state creep. Classical plastic flow theories and power law creep are still widely used. The Anand model unifies both rate-dependent creep (transient creep and steady-state creep) and rate-independent plastic occurring concurrently at the same time in the material. The internal state variable, i.e., the deformation resistance, can represent an averaged isotropic resistance to macroscopic plastic flow. Moreover, it is usually difficult to separate the plastic strain from creep strain to calibrate the parameters of a separated model based on the mechanical experimental tests. The parameters in a unified model can be determined in a direct method combining both rate dependent and rate independent plastic strains into a viscoplastic strain term.

(b) *A creep approximation with hyperbolic form*. It is shown in this paper that the Anand model can be simplified to represent the secondary creep of solders. The creep approximation with hyperbolic form captures the characteristic of the regime of power law breakdown, which may be reached for the corners and interfaces of solder joints under thermal shock and accelerated test conditions. The major deficiency of power law creep models is the lack of predictive power to correctly describe the stress/strain hysteresis loop during thermal cycle loading. The inaccuracy of the hysteresis loop calculation substantially magnifies the error of fatigue life prediction of solder joints.

(c) *Available in commercial finite element code*. There already existed some unified models for solders in electronic packaging, but most of them should provide the time integration scheme and be implemented in the commercial finite element code as user-specified subroutines. Such a work is often complex, expertly dependent, and time-consuming. The rate dependent plasticity in ANSYS code, i.e., the Anand model, provides a useful unified model.

(d) *Iteration stability and lower CPU time-consumption*. As mentioned above, the finite element simulation with the Anand model is more efficient than the creep model.

It should be noted that only a single scalar used to characterize the internal structural characteristics of a material is of course a gross simplification. The Anand model was originally formulated to be used more for hot working process rather than for thermal cyclic loading. Two features for modeling thermal cyclic loading are not considered in the Anand model: (1) kinematic hardening and (2) a thermal (static) recovery term in the evolution equation. Some experiments of the hysteresis loops under isothermal strain fatigue condition (Busso and Kitano [9]) revealed that the solder exhibits the Bauschinger effect. However, modeling the internal mechanisms, which give rise to the macroscopic Bauschinger effect, would require further state variables. In addition, the importance of the Bauschinger effect is somewhat reduced at high homologous temperatures and relatively low strain rate regimes important to solder alloys. The static recovery of solder alloys is still not presently sufficiently studied. Some further studies on the kinematic hardening and the static recovery of solder alloys are needed in the future.

Conclusions

In this paper, a unified viscoplastic constitutive model, the Anand model, which uses a single scalar internal variable to describe the deformation resistance state, was applied to represent the inelastic deformation behavior for solders in electronic packaging. The material parameters of Anand model for 60Sn40Pb, 62Sn36Pb2Ag, 96.5Sn3.5Ag, and 97.5Pb2.5Sn solders were determined from experimental results and separated constitutive relations. The model verifications show that this rate dependent model can excellently reproduce the base and experimental data. Also, a simple application example of simulation on stress/strain responses of solder joints under thermal cycling was presented. It is concluded that the Anand model can be applied for representing the inelastic deformation of solders. This model is useful in finite element simulation of stress/strain responses of solder joints in service.

References

[1] Darveaux, R., and Banerji, K., 1992, ''Constitutive Relations for Tin-Based Solder Joints,'' IEEE Trans. CHMT, **15**, No. 6, pp. 1013–1024.

[2] Weinbel, R. C., Tien, J. K., Pollak, P. A., and Kang, S. K., 1987, ''Creep Fatigue Interaction in Eutectic Lead-Tin Solder Alloys,'' J. Mater. Sci. Lett., **6**, pp. 3091–3096.

[3] Kashyap, B. P., and Murty, G. S., 1981, ''Experimental Constitutive Relations for the High Temperature Deformation of a Pb-Sn Eutectic Alloy,'' Mater. Sci. Eng., **50**, pp. 205–213.

[4] Lau, J., and Rice, J. R., 1990, ''Thermal Stress/Strain Analyses of Ceramic Quad Flat Pack Packages and Interconnections,'' *Proc. Elect. Components and Technology 40th Conf.*, Las Vegas, Nevada, Vol. 1, pp. 824–834.

[5] Sarihan, V., 1993, ''Temperature Dependent Viscoplastic Simulation of Controlled Collapse Solder Joint Under Thermal Cycling,'' ASME J. Electron. Packag., **115**, pp. 16–21.

[6] Pao, Y. H., Badgley, S., Jih, E., Govila, R., and Browning, J., 1993, ''Constitutive Behavior and Low Cycle Thermal Fatigue of 97Sn3Cu Solder Joints,'' ASME J. Electron. Packag., **115**, No. 6, pp. 147–152.

[7] Knecht, S., and Fox, L. R., 1990, ''Constitutive Relation and Creep-Fatigue Life Model for Tin-lead Solder,'' IEEE Trans. CHMT, **13,**, No. 2, pp. 424–433.

[8] Busso, E. P., Kitano, M., and Kumazawa, T., 1994, ''Modeling Complex Inelastic Deformation Processes in IC Packages' Solder Joints,'' ASME J. Electron. Packag., **116**, No. 3, pp. 6–15.

[9] Busso, E. P., and Kitano, M., 1992, ''A Visco-Plastic Constitutive Model for 60/40 Tin-Lead Solder Used in IC Package Joints,'' ASME J. Eng. Mater. Technol., **114**, pp. 331–337.

[10] Qian, Z., and Liu, S., 1997, ''A Unified Viscoplastic Constitutive Model for Tin-Lead Solder Joints,'' *Advances in Electronic Packaging*, ASME EEP-Vol. 19-2, pp. 1599–1604.

[11] Skipor, A. F., et al., 1996, ''On the Constitutive Response of 63/37 Sn/Pb Eutectic Solder,'' ASME J. Eng. Mater. Technol., **118**, pp. 1–11.

[12] Ma, X., Wang, L., Fang, H. Y., and Qian, Y. Y., 1998, ''Bodner-Partom Constitutive Relations for Eutectic Tin-Lead Solder,'' Chinese J. Applied Mechanics, **15**, No. 2, pp. 87–90 (in Chinese).

[13] Weber, G. G., Lush, A. M., Zavaliangos, A., and Anand, L., 1991, ''An Objective Time-Integration Procedure for Isotropic Rate-Independent and Rate-Dependent Elastic-Plastic Constitutive Equations,'' Int. J. Plast., **6**, pp. 701–744.

[14] Anand, L., 1985, ''Constitutive Equations for Hot Working of Metals,'' J. Plasticity, **1**, pp. 213–231.

[15] Brown, S. B., Kim, K. H., and Anand, L., 1989, ''An Internal Variable Constitutive Model for Hot Working of Metals,'' Int. J. Plast., **5**, pp. 95–130.

[16] Garofalo, F., 1963, ''An Empirical Relation Defining the Stress Dependence of Minimum Creep Rate in Metals,'' Trans. AIME, **227**, 351–362.

[17] Arrowood, R., Mukherjee, A., and Jones, W. B., 1991, ''Hot Deformation of Two-Phase Mixtures,'' *Solder Mechanics: A State of the Art Assessment*. Frear, D. R., Jones, W. B., and Kinsman, K. R., eds., TMS, Warrendale, pp. 107–153.

[18] Grivas, D., Murty, K. I., and Morris, J. W., 1979, ''Deformation of Pb/Sn Eutectic Alloys at Relatively High Strain Rates,'' Acta Metall. **27**, pp. 731–737.

[19] Solomon, H. D., 1986, ''Creep, Strain-Rate Sensitivity and Low Cycle Fatigue of 60/40 Solder,'' Brazing and Soldering, **11**, pp. 68–75.

[20] Holden, S. J., and Wallace, E. R., 1999, ''Modeling the Effects of Microstructure in BGA Joints,'' Int. J. Microcircuits Electron. Packag., Second Quarter, **22**, No. 2, pp. 80–85.

[21] Wang, J., Qian, Z., Zou, D., and Liu, S., 1998, ''Creep Behavior of a Flip-Chip Package by Both FEM Modeling and Real Time Moire Interferometry,'' ASME J. Electron. Packag., **120**, pp. 179–185.

[22] Hong, B. Z., and Burrell, L. G., 1997, ''Model Thermally Induced Viscoplastic Deformation and Low Cycle Fatigue of CBGA Solder Joints in a Surface Mount Package, IEEE Trans. CPMT-Part A, **20**, No. 3, pp. 280–285.

[23] Wiese, S., Feustel, F., Rzapka, S., and Meusel, E., 1998, ''′Experimental Characterization of Material Properties of 63Sn36Pb Flip Chip Solder Joints, *Proc. Mat. Res. Soc. Symp*., Vol. 515, pp. 233–238.

[24] Fusaro, J. M., and Darveaux, R., 1997, ''Reliability of Copper Base-plate High Current Power Modules,'', Int. J. Microcircuits Electron. Packag., Second Quarter, **20**, No. 2, pp. 81–88.

[25] Pao, Y. H., Jih, E., Badgley, S., and Browning, J., 1992, ''Thermal Cyclic Behavior of 97Sn-3Cu Solder Joints,'' *ASME 92-WA/EEP-21*, pp. 1–6.

[26] Wilde, J., Cheng, Z. N., and Wang. G. Z., 1999, ''Influences of Packaging Materials on the Solder Joints Reliability of Chip Scale Assemblies,'' *Proc. 1999 Inter. Symp. on Advan. Packag. Mater*., (Braselton, Georgia), pp. 141–149.

[27] Pao, Y. H., Badgley, S., Govila, R., Baumgartner, L., Allor, R., and Cooper, R., 1992, ''Measurements of Mechanical Behavior of High Lead Lead-Tin Solder Joints Subjected to Thermal Cycling,'' ASME J. Electron. Packag., **114**, pp. 135–145.